Carbohydrate Polymers 94 (2013) 339–344

Contents lists available at SciVerse ScienceDirect

Carbohydrate Polymers

journal homepage: www.elsevier.com/locate/carbpol

Sodium alginate/graphene oxide composite films with enhanced thermal and mechanical properties

Mariana Ionita, Madalina Andreea Pandele*, Horia Iovu

University Politehnica of Bucharest, Advanced Polymer Materials Group, 132 Calea Grivitei, 010737, Bucharest, Romania

ARTICLE INFO

Article history:
Received 19 November 2012
Received in revised form 14 January 2013
Accepted 21 January 2013
Available online 4 February 2013

Keywords:
Sodium alginate
Graphene oxide
Film
Mechanical properties

ABSTRACT

Sodium alginate/graphene oxide (Al/GO) nanocomposite films with different loading levels of graphene oxide were prepared by casting from a suspension of the two components. The structure, morphologies and properties of Al/GO films were characterized by Fourier transform infrared (FT-IR) spectroscopy, X-ray diffraction (XRD), scanning (SEM) and transmission electron microscopy (TEM), thermal gravimetric (TG) analysis, and tensile tests. The results revealed that hydrogen bonding and high interfacial adhesion between GO filler and Al matrix significantly changed thermal stability and mechanical properties of the nanocomposite films. The tensile strength (σ) and Young's modulus (E) of Al films containing 6 wt% GO increased from 71 MPa and 0.85 GPa to 113 MPa and 4.18 GPa, respectively. In addition, TG analysis showed that the thermal stability of Al/GO composite films was better than that of neat Al film.

1. Introduction

Alginates as a star in biomaterials research have been attracting tremendous attention in the past few years in various fields of biomedicine (Augst, Kong, & Mooney, 2006). They have been found widespread applications in scaffolds for tissue engineering, delivery vehicles for drugs, and as model extracellular matrices for biological studies (Augst et al., 2006; Hua, Ma, Li, Yang, & Wang, 2010; Rani, Mishra & Sen, 2012; Rowley, Madlambayan, & Mooney, 1999; Tezcan, Gunister, Ozen, & Erin, 2012). Biomaterials for tissue engineering require tight control of a number of properties including mechanical stiffness, maintain physical integrity or bear loads until they are replaced by newly formed tissue, swelling, and cell attachment. Alginates themselves display some unsatisfactory properties such as poor mechanical strength and loss of structural integrity which limits the applications (Rani et al., 2012). Currently, much effort has been made for improving the performance of alginates tissue engineering scaffolds. Compounding of alginates with other polymers such as pectin (Beyer, Reichert, Heurich, Jandt, & Sigusch, 2010), chitosan (Li, Ramay, Hauch, Xiao, & Zhang, 2005), or polyvinyl alcohol (Bichara et al., 2010) has been found to provide just marginal effect. Successful attempts involved the embedding of alginates with inorganic materials. Carbon nanotubes reinforced alginates scaffolds are mechanically strong and electro-active which is useful for stimulate-guided growth cells (Kawaguchi et al., 2006). However, the techniques utilized in carbon nanotubes fabrication involve the use of metal catalyst which can be trapped inside carbon nanotubes and its presence introduces significant toxicity (Ge et al., 2008; Pumera, 2007). Graphene/graphene oxide (GO) material has become one of the most fascinating materials in the past few years in various fields including biomedicine (Bao et al., 2011; Rodrigue-Gonzalez et al., 2012; Zhu et al., 2010). GO is essentially a sheet that is only one atom thick with large specific surface area and a large number of functional groups (*e.g.* hydroxyl, epoxide, and carbonyl groups) bound on the surface. The chemical groups of GO have been found to be an effective means to impart the desired solubility in water or different solvents (Zhu et al., 2010). Moreover, these functional groups improve interfacial interaction between graphene oxide and a polymer matrix and pave the pathways for developing GO based nanocomposites with remarkable mechanical and thermal properties (Meyer et al., 2007). Recent prominent studies have explored GO potential the make functional biomaterials. Han, Yan, Chen, and Li (2011) reported a significant, simultaneous, improvement of strength and toughness of chitosan with incorporation of 1 wt% GO. Fan et al. (2010) reported a significant increase (over 200%) of elastic modulus of chitosan with the addition of small amount of graphene (0.1–0.3 wt%) furthermore the GO based composites were noncytotoxic. Gelatin–GO films with improved bioactivity and mechanical response were prepared (Wan, Frydrych, & Chen, 2011). However, to the best of our knowledge, there have been no previous reports on the possibility of alginate (Al) embedded with graphene or GO. GO sheet presents numerous oxygen functional groups in the basal planes and the borders which could allow homogeneous distribution of GO sheets and generate interfacial bonding with hanging

* Corresponding author. Tel.: +40 745266484.
E-mail addresses: andreeamadalina.pandele@yahoo.com, doggo_rom@yahoo.com (M.A. Pandele).

0144-8617/$ – see front matter © 2013 Elsevier Ltd. All rights reserved.
http://dx.doi.org/10.1016/j.carbpol.2013.01.065

hydroxyl groups of Al, and thus take advantage of the excellent properties of GO material.

In the present study, we employed casting techniques for the preparation of novel Al/GO nanocomposite films and then structural, morphological, thermal stability and mechanical properties of the films were explored. The addition of 6 wt% GO significantly improved the Young's modulus by about 300% and increased the thermal stability of Al/GO composite films with about 25 °C.

2. Experimental

2.1. Materials

High-purity graphene oxide was kindly supplied by National Institute for Research and Development in Microtechnologies (Romania). They were manufactured from natural graphite by Hummer's method (Obreja et al., 2011; William, Hummers, & Richard, 1958). Alginic acid sodium salt from brown algae with medium viscosity was purchased from Sigma–Aldrich. All materials were used without future purification.

2.2. Preparation of graphene oxide-based sodium alginate composite films

Graphene oxide aqueous suspensions were prepared by ultrasonic treatment using double distillate (DD) water. Briefly, 0.1 g of GO was mixed in 100 ml of DD water. The mixture was sonicated for 1 h to get a homogenous dispersion. The alginate solution was obtained by dissolving the sodium alginate in DD water as 1% (w/v) solution. Composite films with different GO contents (0, 0.5, 1, 2.5, and 6 wt%) were produced by drop wise GO suspension to the sodium alginate solution. The resulting mixture was constantly stirred for about 30 min using a magnetic stirrer. Each solution was cast onto transparent glass Petri dish and left undisturbed for 72 h at ambient temperature allowing formation of thin film. The films were peeled off from the mould and then thermal treated to a *vacuum* pressure of 80 kPa according to the following procedure: 30 min 50 °C, 30 min 70 °C and 4 h at 120 °C.

2.3. Characterization

The structural characteristics of the films were studied by X-ray diffraction (XRD) using Panalytical X'Pert Pro MPD instrument with Cu Kα radiation. Fourier transform infrared (FT-IR) spectra were recorded on a Bruker VERTEX 70 spectrometer using 32 scans with a resolution of 4 cm^{-1} in 4000–600 cm^{-1} region. The samples were analysed from ATR. To investigate Al/GO composites by transmission electron microscopy (TEM) small pieces of the films were embedded in an Epon resin, cut on microtome, transferred to a copper grid covered with a thin amorphous carbon films with holes. TEM images were recorded on TECNAI F30 G2 S-TWIN equipment provided with 300 kV emission gun. The surface morphology of Al/GO composite films was characterized by field-emission scanning electron microscope (SEM; QUANTA INSPECT F) with 1.2 nm resolution and an energy dispersive X-ray spectrometer with resolution of 133 eV to MnKα. Thermogravimetric (TG) analysis was done on a Q 500 TA Instrument. The samples of 1.5 mg were heated from 30 to 620 °C at a scanning rate of 10 °C/min under a constant nitrogen flow rate (40 mL/min).

Mechanical test was performed using an universal mechanical tester (Instron, Model 3382, USA) at a speed of 2 mm/min at room temperature and relative humidity was 45–50%. The size of the test specimens was 10 cm in length and 1 cm in width. A minimum of ten specimens were tested for each sample and the average values are reported.

Table 1
XRD data of Al and Al/GO nanocomposite films.

Sample	FWHM [°]	2θ [°]	ds [Å]
Al	3.24	13.32	6.63
GO	2.26	10.92	8.06
Al/GO 0.5 wt%	3.37	5.02	17.73
		13.46	6.71
Al/GO 1 wt%	3.67	5.07	17.42
		13.59	6.51
Al/GO 2.5 wt%	4.00	5.13	17.19
		13.36	6.62
Al/GO 6 wt%	4.00	5.69	15.51
		13.31	6.65

3. Results and discussion

By employing casting technique well-dispersed Al/GO nanocomposite films were fabricated with thickness of 70 ± 10 μm. Because of the oxygen functional groups on the surface of the GO sheets, these were dispersed at the level of individual sheets.

3.1. FT-IR studies

FT-IR experiments were carried out to investigate the interaction between GO and Al. Fig. 1 shows absorption bands from FT-IR spectrum of Al, GO and Al/GO composite films. The FT-IR spectrum of GO and Al were similar to those previously presented in literature (Li et al., 2012; Malesu, Sahoo, & Nayak, 2011). In the Al spectrum the peak at 3347 cm^{-1} is attributed to OH stretching vibration, the bands at 1600 cm^{-1} and 1414 cm^{-1} correspond to symmetric and asymmetric COO^- stretching vibration of carboxylate salt group, and the peak at 1030 cm^{-1} is assigned to the stretching vibration of C—O—C— groups respectively (Malesu et al., 2011). For the GO spectrum, dominant peaks appear at 3401 cm^{-1}, 1735 cm^{-1}, 1624 cm^{-1}, 1043 cm^{-1} and are assigned to OH stretching vibration, C═O stretching vibration of the carboxylic group, C═C stretching mode of the sp^2 network and C—O stretching vibration respectively (Li et al., 2012), demonstrating the presence of the reactive groups in the GO product.

From FT-IR spectrum of the composite films a shoulder peak at 1735 cm^{-1} due to the carboxyl groups from the GO surface can be observed, in addition to Al spectrum, which evidences the presence of GO in composite films. Moreover with the GO addition, the peaks at 3347 and 3401 cm^{-1} (O—H stretching vibration) broadened and shifts to smaller wavelengths (3331 cm^{-1}) which can be attributed to the interaction of Al and GO through intermolecular hydrogen bonds. The achieved electrostatic attraction and hydrogen bonding between Al and GO may induced good interfacial adhesion at the interface GO/Al and result in an enhanced mechanical response.

3.2. XRD studies

Fig. 2 depicts the X-ray diffractograms of Al, GO, and Al/GO composite films with 1 and 2.5 wt% GO measured at 25 °C. As shown in Fig. 2A and Table 1, GO spectrum exhibits a characteristic peak at $2\theta = 10.92°$ and the d spacing obtained from Bragg equations as 8.06 Å, which is within the range of values that has been previously reported (Jingchao, Xianbao, Chunhui, Min, & Xiaopen, 2011). Conversely, in the XRD pattern of Al film the weak, broad diffraction peak at 13.32°, with average intermolecular distance 6.63 Å indicates a rather amorphous structure for this compound (Kim, Lim, Jegal, & Lee, 2000). All of the XRD patterns of the composite films present two diffraction peaks at $2\theta \sim 5°$ and 13° associated with GO and Al respectively. The diffraction angle characteristic for GO is shifted toward lower angle values (Table 1) and the GO interlayer spacing increases from 8.06 Å for pristine GO to ~17 Å for Al/GO

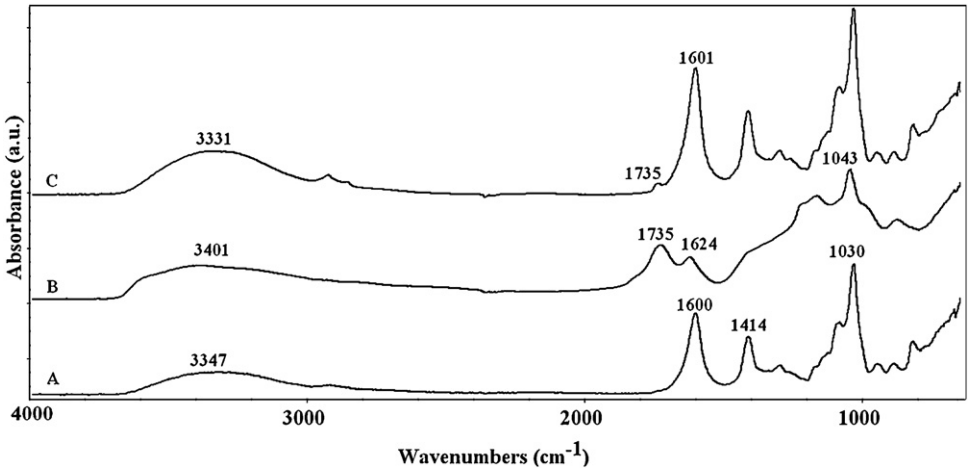

Fig. 1. FT-IR spectra of (A) Al, (B) GO, and (C) Al/GO composite film.

composite film with 2.5 wt% GO, indicating formation of intercalated structures. It is noticed that the incorporation of GO within Al matrix slightly broadened the diffraction peak at about 13° indicating that GO is slightly hindering the relatively ordered arrangement of the Al. However the Al structure was not significantly affected by the incorporation of GO indicating that there were mainly physical interaction between Al and GO (Han et al., 2011).

3.3. TEM and SEM studies

Fig. 3 shows typical TEM micrographs of the nanocomposite films Al/GO displaying that GO are indeed present and partially exfoliated into individual sheets within Al matrix. Apparently, GO sheets were unidirectionally distributed in the Al matrix.

To further determine the quality of the GO dispersion and the composite films morphology SEM was employed. Fig. 4 illustrates images of Al and Al/GO composite films with 2.5 wt% GO loading. From the films surface micrographs (Fig. 4A and B) noticeable difference between pure Al and Al/GO composite films can be observed. The surface of Al film displays a homogeneous, smooth morphology (Fig. 4A). Changes in surface morphology were observed for the composite films Al/GO, these revealed a rather rough morphology with some salient banded structures which might be attributed to the GO sheets embedded into Al, there were also few GO sheets dragged out (pointed by black arrows in Fig. 4B. The cross section of the Al/GO composite films is totally different with that of the pristine Al. As shown in Fig. 4D the films became coarser when GO is added with grooves which might be generated by the different structures and stiffness between Al and GO when the films are snapped (Han et al., 2011). Fig. 4D also indicates the well dispersed status of the GO in the Al matrix without any aggregation, in addition, clear stratification of GO parallel to the surface of the film is observed. The alignment of GO sheets is exactly in agreement with TEM assessment. The same observations were reported in the literature for similar materials (*i.e.* chitosan–GO) prepared from the same method (*i.e.* solution casting). Pan, Wu, Bao, and Li (2011), reported that GO sheets tend to lie down inside the chitosan solution due to their 2D structure and gravitational attraction. On the basis of XRD, TEM and SEM results and similar phenomenon found in the preparation of comparable materials (Han et al., 2011; Pan et al., 2011; Yang, Tu, Li, Shang, & Tao, 2010) we propose a possible structure of the Al/GO composite materials. Scheme 1 depicts GO sheets unidirectionally alignment and uniform intercalated with Al chains, "brick-and-mortar" structure

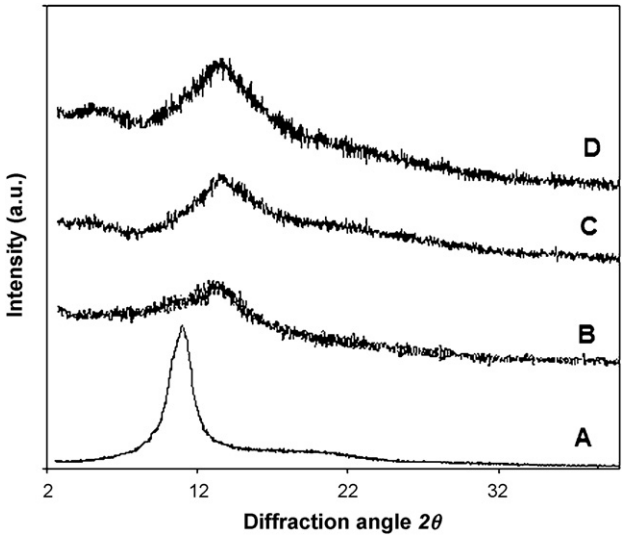

Fig. 2. XRD patterns of (A) GO, (B) Al, (C) Al/GO 1 wt% and (D) Al/GO 2.5 wt% films.

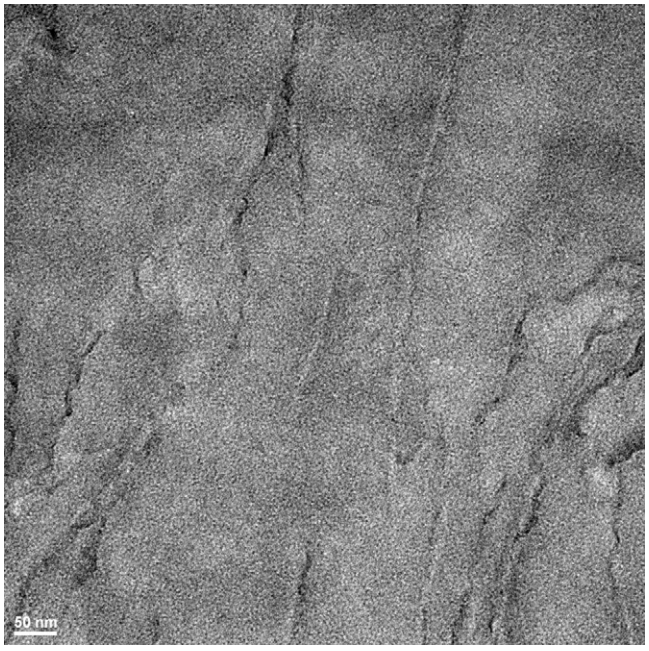

Fig. 3. TEM images of Al/GO 2.5 wt% composite films.

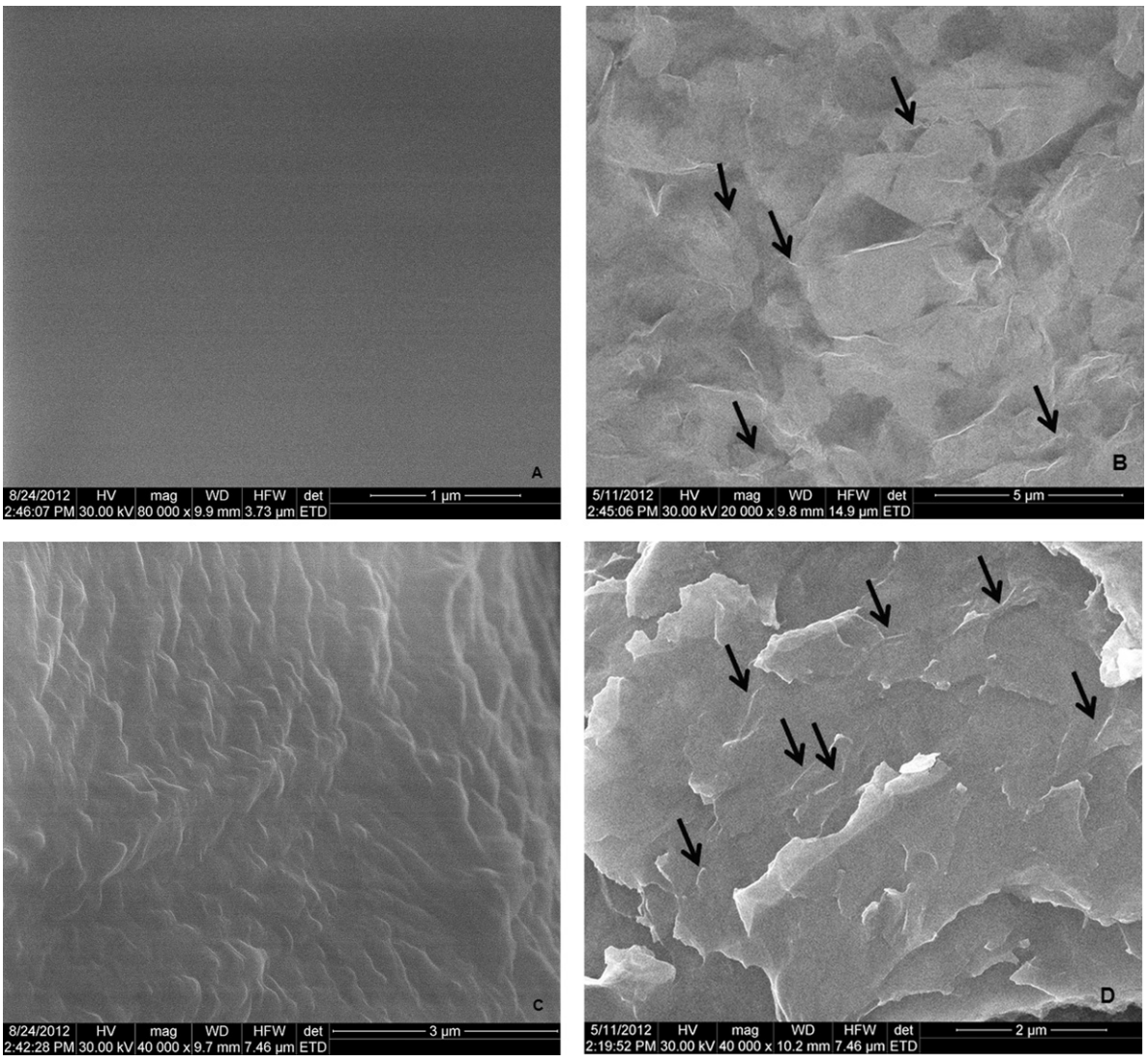

Fig. 4. SEM film surface images (A, B) and fracture surface images (C, D) of (A, C) Al and (B, D) Al/GO 2.5 wt%.

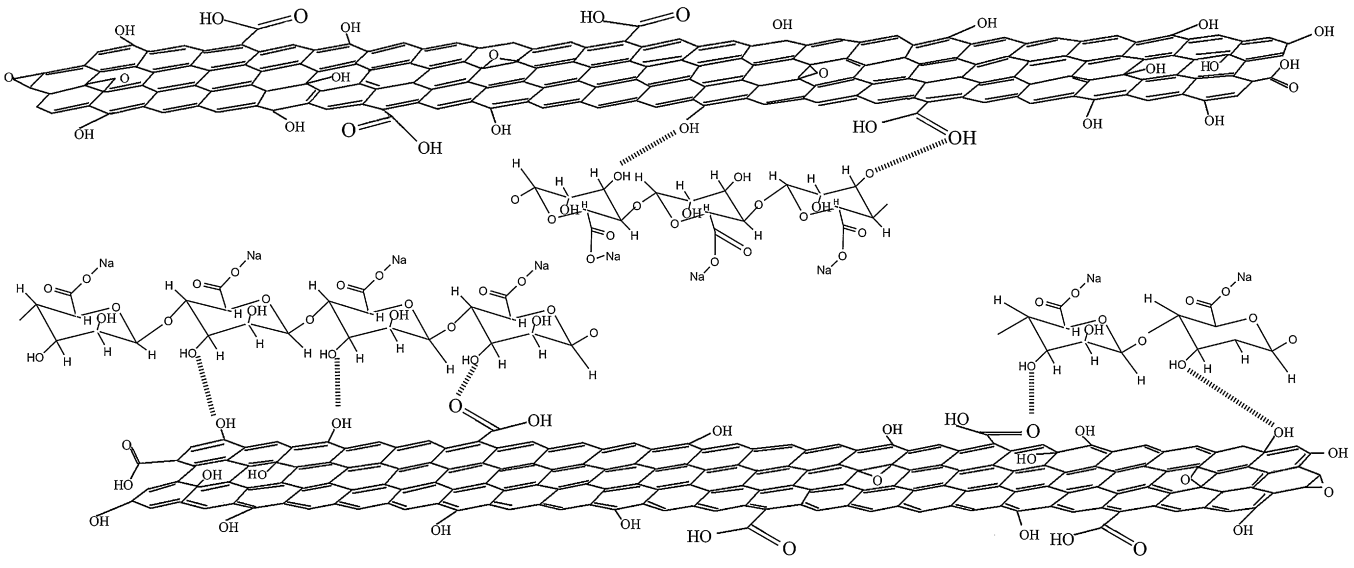

Scheme 1. Schematic representation Al/GO nanocomposite films structure.

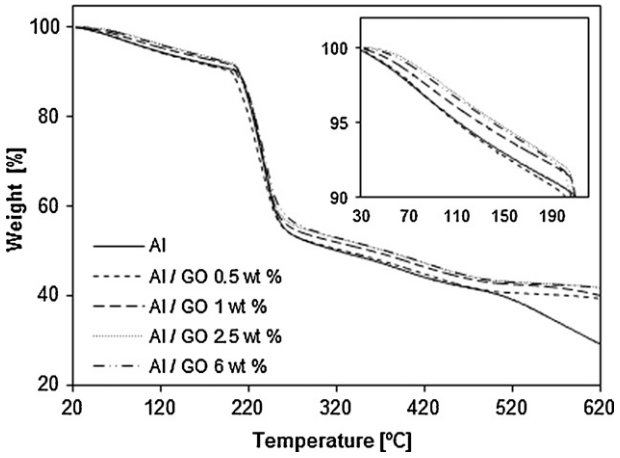

Fig. 5. TG analysis curves of neat Al and Al/GO composite films. Inset: magnification of first stage of degradation.

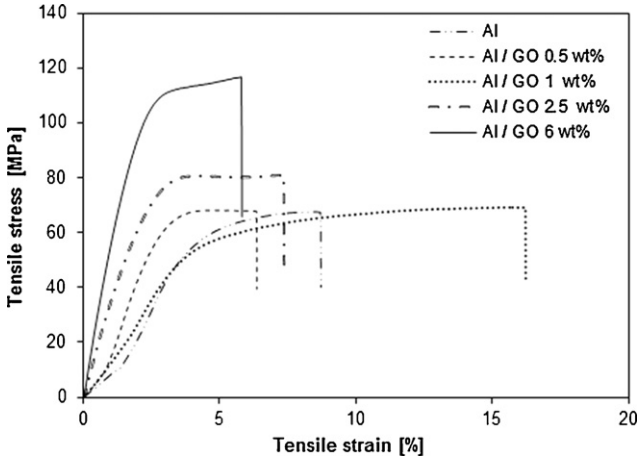

Fig. 6. Tensile stress *versus* strain curves for Al and Al/GO films as a function of GO content.

Table 2
Decomposition temperature and mechanical properties of neat Al and Al/GO nanocomposite films.

Sample	$Td_{3\%}$ [a] [°C]	Tensile modulus [GPa]	Tensile strength [MPa]
Al	80	0.85 ± 0.08	71 ± 9
Al/GO 0.5 wt%	81	1.45 ± 0.42	68 ± 5
Al/GO 1 wt%	94	1.39 ± 0.52	82 ± 1
Al/GO 2.5 wt%	108	3.80 ± 0.47	86 ± 4
Al/GO 6 wt%	105	4.18 ± 0.11	113 ± 4

[a] The temperature at which the weight loss is 3%.

(Yang et al., 2010). FT-IR results suggested the possible formation of hydrogen bonds between Al and GO oxygen functional groups as schematically shown in Scheme 1, but additional work is needed to investigate this feature. The homogeneous uniform dispersion and certain degree of alignment of GO within Al matrix coupled with good interfacial adhesion between GO and Al should lead to significant improvement in thermal stability and mechanical properties of Al/GO nanocomposite films.

3.4. TG studies

The TG analysis of Al/GO composite films shows higher starting decomposition temperature around 100 °C and less weight loss than that of pure Al films (Fig. 5 and Table 2). The temperature at which the weight loss is 3% ($Td_{3\%}$) increased by about 30 °C in the case of the composite with the highest amount of GO added to the pure biopolymer. Conversely, the residual weight loss of the composites is higher than that of neat Al, which can be attributed to the excellent thermal stability of GO which generally present a decomposition temperature around 200 °C (Qiu et al., 2011).

3.5. Mechanical properties investigation

Eventually, the mechanical behavior of the films, pure Al and Al/GO composites was investigated by tensile tests. Fig. 6 shows typical stress–strain curves of neat Al and its composites with GO. The tensile strength and modulus as a function of GO content are summarized in Table 2. The data are the average results measured for ten samples. Generally a reinforcement of the Al was observed with the addition of the GO. The reinforcement was related to the GO amount, it is evident that even a small amount of GO significantly increases the tensile modulus of Al biopolymer. Moreover, higher values of GO loading from 2.5 to 6 wt% cause a significant increase of tensile strength and Young's modulus from 82 to 113 MPa and from 1.39 to 4.18 GPa respectively. The improvement of the mechanical properties of the composites is mainly attributed to alignment, compatibility and specific interactions of Al hydroxyl groups with GO functional groups (hydroxyl, epoxide) rather than to Al crystallinity modification. In general, as polymer crystallinity decreases, also its level of secondary bonding does and leads to a decline the stiffness and strength of the polymer (Ramkumar & Bhattacharya, 1997). As shown in XRD patterns in Fig. 2, the addition of GO affects only slightly the crystalline structure of Al therefore here the crystallinity plays a less important role. The phenomenon may be explained by the fact that macroscopic properties such as tensile strength are relatively insensitive to small changes in the crystallinity of the composites (Ramkumar & Bhattacharya, 1997). The same observations were reported in the literature for chitosan associated with GO. Yang et al. (2010), reported that the addition of 0.5 wt% GO in the composite films, slightly affects their crystallinity and significant increase the strain modulus, Young's modulus and elongation at break. In this case, the improved tensile properties are ascribed to GO and Al hydrogen bonding and preferential alignment of GO shown by SEM and TEM investigation. As schematically shown in Scheme 1, the brick and mortar structure of the Al/GO composites leads to more uniform stress distribution and minimizes the presence of stress concentration center, thus significantly increase the mechanical properties of the nanocomposite films.

4. Conclusion

This work confirms that high performance Al/GO nanocomposite films could be successfully prepared using a simple solution casting method. FT-IR and XRD results suggested that GO sheets, containing abundant functional groups on the surface, form interaction with the Al matrix. In addition, TEM and SEM evidenced an uniform distribution and preferential alignment of GO sheets within Al matrix. The incorporation of GO sheets within Al matrix have beneficial effect on mechanical integrity and thermal stability of the nanocomposite films. Among the studied nanocomposite films Al/GO with 6 wt% GO exhibited the highest increase of the tensile strength and Young's modulus from 71 to 113 MPa and from 0.85 GPa to 4.18 GPa respectively. Meanwhile, the TG analysis indicate that the incorporation of 6 wt% GO in the Al matrix leads to an increase of $Td_{3\%}$ with about 25 °C.

Acknowledgements

This research has been supported by the National Research Grant PN-II-PCCA-140, CNCS-UEFISCDI.

References

Augst, A. D., Kong, H. J., & Mooney, D. J. (2006). Alginate hydrogels as biomaterials. *Macromolecular Bioscience*, *6*(8), 623–633.

Bao, H., Pan, Y., Ping, Y., Sahoo, N. P., Wu, T., Li, L., et al. (2011). Chitosan-functionalized graphene oxide as a nanocarrier for drug and gene delivery. *Small*, *7*(11), 1569–1578.

Beyer, M., Reichert, J., Heurich, E., Jandt, K. D., & Sigusch, B. W. (2010). Pectin, alginate and gum arabic polymers reduce citric acid erosion effects on human enamel. *Dental Materials Journal*, *26*(9), 831–839.

Bichara, D. A., Zhao, X., Hwang, N. S., Bodugoz-Senturk, H., Yaremchuk, M. J., Randolph, M. A., et al. (2010). Porous poly(vinyl alcohol)-alginate gel hybrid construct for neocartilage formation using human nasoseptal cells. *Journal of Surgical Research*, *163*(2), 331–336.

Fan, H., Wang, L., Zhao, K., Li, N., Shi, Z., Ge, Z., et al. (2010). Fabrication, mechanical properties, and biocompatibility of graphene-reinforced chitosan composites. *Biomacromolecules*, *11*(9), 2345–2351.

Ge, C., Lao, F., Li, W., Chen, C., Qui, Y., Mao, X., et al. (2008). Quantitative analysis of metal impurities in carbon nanotubes: Efficacy of different pretreatment protocols for ICPMS Spectroscopy. *Analytical Chemistry*, *80*(24), 9426–9434.

Han, D., Yan, L., Chen, W., & Li, W. (2011). Preparation of chitosan/graphene oxide composite film with enhanced mechanical strength in the wet state. *Carbohydrate Polymers*, *83*(2), 653–658.

Hua, S., Ma, H., Li, X., Yang, H., & Wang, A. (2010). pH-sensitive sodium alginate/poly(vinyl alcohol) hydrogel beads prepared by combined Ca^{2+} crosslinking and freeze-thawing cycles for controlled release of diclofenac sodium. *International Journal of Biological Macromolecules*, *46*(5), 517–523.

Jingchao, W., Xianbao, W., Chunhui, X., Min, Z., & Xiaopen, S. (2011). Preparation of graphene/poly(vinyl alcohol) nanocomposites with enhanced mechanical properties and water resistance. *Polymer International*, *60*(5), 816–822.

Kawaguchi, M., Fukushima, T., Hayakawa, T., Nakashima, N., Inoue, Y., Takeda, S., et al. (2006). Preparation of carbon nanotube-alginate nanocomposite gel for tissue engineering. *Dental Material Journal*, *25*(4), 719–725.

Kim, S. G., Lim, G. T., Jegal, J., & Lee, K. J. (2000). Pervaporation separation of MTBE (methyl tert-butyl ether) and methanol mixtures through polyion complex composite membranes consisting of sodium alginate/chitosan. *Journal of Membrane Science*, *174*(1), 1–15.

Li, L., Li, C., Qiong, J., Pengfei, X., Xiaoting, L., & Qiuping, Z. (2012). Preparation and characterization of chitosan/graphene oxide composites for the adsorption of Au (III) and Pd(II). *Talanta*, *93*, 350–357.

Li, Z., Ramay, H. R., Hauch, K. D., Xiao, D., & Zhang, M. (2005). Chitosan–alginate hybrid scaffolds for bone tissue engineering. *Biomaterials*, *26*(18), 3919–3928.

Malesu, V. K., Sahoo, D., & Nayak, P. L. (2011). Chitosan–sodium alginate nanocomposites blended with cloisite 30B as a novel drug delivery system for anticancer drug curcumin. *International Journal of Applied Biology and Pharmaceutical Technology*, *2*(3), 402–411.

Meyer, J. C., Geim, A. K., Katsnelson, M. I., Novoselov, K. S., Booth, T. J., & Roth, S. (2007). The structure of suspended graphene sheets. *Nature*, *446*, 60–63.

Obreja, A. C., Cristea, D., Gavrila, R., Schiopu, V., Dinescu, A., Danila, M., et al. (2011). Functionalized graphene/poly 3-hexyl thiophene based nanocomposites. In *Proceedings of IEEE International Semiconductor Conference CAS* Sinaia, Romania, (pp. 27–30).

Pan, Y., Wu, T., Bao, H., & Li, L. (2011). Green fabrication of chitosan films reinforced with parallel aligned graphene oxide. *Carbohydrate polymers*, *83*(4), 1908–1915.

Pumera, M. (2007). Carbon nanotubes contain residual metal catalyst nanoparticles even after washing with nitric acid at elevated temperature because these metal nanoparticles are sheathed by several graphene sheets. *Langmuir*, *23*(11), 6453–6458.

Qiu, S. L., Wang, C. S., Wang, Y. T., Liu, C. G., Chen, X., Xie1, H. F., et al. (2011). Effects of graphene oxides on the cure behaviors of a tetrafunctional epoxy resin. *Polymer Letters*, *5*(9), 809–818.

Ramkumar, D. H. S., & Bhattacharya, M. (1997). Effect of crystallinity on the mechanical properties of starch/synthetic polymer blends. *Journal of Materials Science*, *32*(10), 2565–2572.

Rani, P., Mishra, S., & Sen, G. (2012). Microwave based synthesis of polymethyl methacrylate grafted sodium alginate: its application as flocculant. *Carbohydrate Polymers*, *91*(2), 682–685.

Rodrigue-Gonzalez, C., Martinez-Hernandez, A. L., Castano, V. M., Kharissova, O. V., Ruoff, R. S., & Velasco-Santos, C. (2012). Polysaccharide nanocomposites reinforced with grapheme oxide and keratin-graphene oxide. *Industrial & Engineering Chemistry Research*, *51*(9), 3619–3629.

Rowley, J. A., Madlambayan, G., & Mooney, D. J. (1999). Alginate hydrogel as synthetic extracellular matrix materials. *Biomaterials*, *20*(1), 45–53.

Tezcan, F., Gunister, E., Ozen, G., & Erin, F. B. (2012). Biocomposite films based on alginate and organically modified clay. *International Journal of Biological Macromolecules*, *50*(4), 1165–1168.

Wan, C., Frydrych, M., & Chen, B. (2011). Strong and bioactive gelatin–graphene oxide nanocomposites. *Soft Matter*, *7*(13), 6159–6166.

William, S., Hummers, J., & Richard, E. (1958). Preparation of graphitic oxide. *Journal of American Chemical Society*, *80*(6), 1339.

Yang, X., Tu, Y., Li, L., Shang, S., & Tao, X. (2010). Well-dispersed chitosan/graphene oxide nanocomposites. *Applied Materials Interfaces*, *2*(6), 1707–1713.

Zhu, Y., Murali, S., Cai, W., Li, X., Suk, J. W., Potts, J. R., et al. (2010). Graphene and graphene oxide: Synthesis, properties, and applications. *Advanced Materials*, *22*(35), 3906–3924.